CrossMark
[Click for updates](#)

Aerosol Science and Technology
Publication details, including instructions for authors and subscription information:
http://www.tandfonline.com/loi/uast20

The Influence of Fiber Geometry and Orientation Angle on Filtration Performance

Kun Wang[a] & Haibo Zhao[a]
[a] State Key Laboratory of Coal Combustion, Huazhong University of Science and Technology, Wuhan, Hubei, People's Republic of China
Accepted author version posted online: 06 Jan 2015.Published online: 05 Feb 2015.

To cite this article: Kun Wang & Haibo Zhao (2015) The Influence of Fiber Geometry and Orientation Angle on Filtration Performance, Aerosol Science and Technology, 49:2, 75-85, DOI: 10.1080/02786826.2014.1003278

To link to this article: http://dx.doi.org/10.1080/02786826.2014.1003278

Aerosol Science and Technology, 49:75–85, 2015

ISSN: 0278-6826 print / 1521-7388 online
DOI: 10.1080/02786826.2014.1003278

The Influence of Fiber Geometry and Orientation Angle on Filtration Performance

Kun Wang and Haibo Zhao
State Key Laboratory of Coal Combustion, Huazhong University of Science and Technology, Wuhan, Hubei, People's Republic of China

In this article, the particle filtration processes of five noncircular fibers with triangular, quatrefoil, trilobal, rectangular, and elliptical cross-sections were numerically investigated, and the pressure drop, capture efficiency, and quality factor due to three main capture mechanisms (diffusion, interception, and inertial impaction) were calculated. By comparing the results with circular fiber, which has the same volume fraction as the five noncircular fibers, the following results can be found. The diffusional capture efficiency, which is highly dependent on the superficial area of fibers, is almost independent of the orientation angle for all fibers. For the quatrefoil, trilobal, and elliptical fibers, as the aspect ratio of component ellipse increases, the capture range also increases, as does the capture efficiency due to three different mechanisms. When considering submicron particles with medium size, which are difficult to capture with circular fibers (especially when dominated by the interception mechanism), triangle and trilobal fibers have higher capture efficiency when the orientation angle is 0° and 60°, respectively. The quality factors of these fibers due to the three capture mechanisms were also investigated in this article. The triangular and rectangular fibers placed horizontally perform better for intermediate and high-inertia particles, and the elliptical fiber placed horizontally shows an advantage in capturing small particles with strong Brownian diffusion.

1. INTRODUCTION

Compared with a traditional electrostatic precipitator, filtration has the advantage of higher capture efficiency of submicron particles. Fiber filtration is involved in complicated particle-flow-fiber interactions and various particle capture mechanisms (Brownian diffusion, interception, inertial impaction, electrostatic attraction, gravitational settling, and so on). Over the past 50 years, many researchers have investigated the filtration process of filters composed of cylindrical fibers through theoretical analysis, numerical simulation, and experimental measurement (Brown 1993). Some analytical/semiempirical/empirical expressions for the capture efficiency and drag force (pressure drop) of circular cross-section fibers were proposed. Such studies include, but are not limited to, the analytical solution of flow filed around a circle of Kuwabara (1959) and Happel (1959), the pressure drop (dimensionless drag force) of Kirsch and Fuchs (1967), capture efficiencies due to Brownian diffusion, interception, and inertial impaction of Stechkina and Fuchs (1966), Kirsch and Fuchs (1968), Stechkina et al. (1969), Lee and Liu (1981), Lee and Liu (1982), and Liu and Wang (1997).

With the recent advancements in fiber manufacturing technology, the production of synthetic fibers with various cross-sections, such as square, rectangle, ellipse, quatrefoil, triangle, and trilobal, is becoming increasingly viable. Relatively, there are very few studies on the pressure drop and capture efficiency of noncircular fibers. Nearly all of these studies are based on theoretical analysis and numerical simulation. Brown (1984) first investigated the flow fields and pressure drop of parallel square multifibers. Fardi and Liu (1992a,b) investigated the pressure drop of rectangular fiber and the capture efficiency dominated by Brownian diffusion and interception for the first time. Wang (1996) used the eigenfunction expansion and domain decomposition method to study the Stokes flow fields around multilayer rectangular fibers and proposed an empirical formula to calculate the drag force of single square cross-section fiber. Adamiak (1999) used the finite element method to analyze the capture process of square fiber in an electric field and explored the influence of Stokes number, Reynolds number, and the quantity of electric charge on a particle's motion and capture efficiency. Ouyang and Liu (1998) analyzed the flow fields and pressure drop of rectangular fiber by solving the biharmonic equation of stream function for various fiber aspect ratios and packing density under continuum and slip boundary conditions. Zhu et al. (2000) focused on the filtration process of rectangular cross-section fiber dominated by the inertial impaction mechanism. Dhaniyala (1999) investigated the dimensionless drag force of three-dimensional square cross-section multifibers using a finite volume approach

Received 19 July 2014; accepted 21 December 2014.
Address correspondence to Haibo Zhao, State Key Laboratory of Coal Combustion, Huazhong University of Science and Technology, Luoyu Road 1037, Wuhan 430074, Hubei, People's Republic of China. E-mail: klinsmannzhb@163.com
Color versions of one or more of the figures in the article can be found online at www.tandfonline.com/uast.

and evaluated the effects of interfiber distance and packing density distribution on the drag force. Cao et al. (2004) numerically studied the trajectory and capture efficiency of neutral/singly charged particles through the staggered parallel rectangular charged fibers, considering the effects of aspect ratio of rectangular fiber on filtration. Cheung et al. (2005) simulated the filtration efficiency and particle loading process of electret split type rectangular fibers.

In terms of elliptical fibers, there are limited studies on the flow fields, capture efficiency, and pressure drop. Here we quote the studies of Raynor (2002) and Kirsh (2011) for flow fields and pressure drop and Raynor (2008), Regan and Raynor (2009) and Wang et al. (2012b) for diffusional and interceptive efficiencies of single elliptical fiber. Recently, Wang et al. (2014) in our research group obtained a series of empirical correction factors for the pressure drop and capture efficiency of elliptical fiber from the existing formulas of circular fiber.

Other noncircular fibers have rarely been studied in terms of flow fields, capture efficiency, and pressure drop. Lamb and Costanza (1980) examined the capture efficiency of fibers having three or four lobes through a theoretical analysis and experimental methods and proved that their filtration performance was better than that of circular fiber. Sanchez et al. (2007) compared the collection efficiency of coal fly ash particles and the pressure drop of trilobal polyimide fibers with circular polyester fibers through experimental measurements and discovered that the collection efficiency of polyimide fiber filters is higher than that of polyester, and the pressure drop showed an opposite variation. Hosseini and Tafreshi (2011) investigated numerically the effects of fibers' cross-sectional shape (circle, square, trilobal, and ellipse) on the performance of a fibrous filter in the slip (nanofibers) and no-slip (microfibers) flow regimes. They found that fiber geometry is more sensitive to pressure drop rather than capture efficiency. Inagaki et al. (2001) numerically and experimentally studied the diffusional collection efficiency of I-, Y-, and H-shaped fibers. However, their numerical method could not address the interception filtration problems.

All these works that referred to noncircular fibers proved that the fibers' cross-sectional shape has a significant influence on the pressure drop and capture efficiency of the fibrous filter. Generally speaking, fibers with a noncircular cross-section could offer a larger surface area per unit volume than the circular fibers that are usually used, and thus, have performance advantages in the capture efficiency of submicron particles over circular fibers. On one hand, noncircular fibers usually have less streamlined shapes and exhibit much larger drag forces than circular fibers. Although these existing studies, which are usually based on complicated calculations or simulations, could understand the filtration feature of one type of noncircular fiber, comparative study among various noncircular fibers to achieve a rational design for fiber geometry is rare. On the other hand, not only the shape of the cross-section but also the fiber arrangement (e.g., orientation angle of the cross-section to the incoming air flow) influences the capture efficiency and pressure drop as well as the quality factor. Therefore, there is an opportunity to rationalize the shape and orientation angle of the cross-section of noncircular fibers to achieve an optimal performance of fiber filtration in different operating conditions. To the best of our knowledge, there is no study that considers the comprehensive influence of the fiber's cross-sectional shape and orientation angle on the filtration performance of differentially sized particles dominated by various capture mechanisms (Brownian diffusion, interception, and inertial impaction here). It is the main objective of this study.

Our group (Wang et al. 2012a, 2013) has established a Lattice Boltzmann-Cellular Automata (LB-CA) probabilistic model for particle-laden flows. By computing the probability of movement of solid particles on the same regular lattices as fluid, we can quantitatively describe the detailed motion of particles under the combined effects of drag force and Brownian diffusion. In terms of the fluid, we adopted the conventional Lattice Boltzmann method (LBM) to obtain the flow fields. The outstanding advantages of the LBM, compared with general numerical methods include its simple and clear physical pictures, inherent parallelism, and high capability to address complex boundary conditions, making it particularly suitable for describing the filtration of noncircular fibers with, for example, a trilobal cross-section. In the previous work, we have used the LB-CA probabilistic model to simulate the particle filtration process of elliptical fiber (Wang et al. 2014). In the current study, we use the same LB-CA model to simulate the filtration processes of four noncircular fibers with triangular, rectangular, trilobal, and quatrefoil cross-sections. The details of the LB-CA model are not shown here. The capture efficiency, pressure drop, and quality factor of the four noncircular fibers with different orientation angles and aspect ratios are simulated to explore and compare the influences of the fibers' geometry and arrangement on these important filtration parameters. The simulation results of elliptical fiber filtration are not repeatedly presented here, however the elliptical fiber case is compared with other cases to gain a comprehensive understanding of the filtration feature of these noncircular fibers. The fundamental study can serve as the basis of the design and optimization of fibrous filters.

This article is organized as follows. First, the calculation conditions, including the fibers' arrangements, computational domain, boundary conditions, and particle properties, are presented in Section 1. In Section 2, we show the simulation results of the capture efficiency and pressure drop of four noncircular fibers (triangular, rectangular, trilobal, and quatrefoil). These capture efficiencies and pressure drops are compared with those of circular fibers to examine their advantages and disadvantages relative to regular circular fibers. In Section 3, as a general and comprehensive filtration performance index, the quality factors (or the figure of merit) of five noncircular fibers are calculated and compared with each other. From these comparisons, it is possible to conclude which fiber geometry and which orientation angle could be combined to achieve a better filtration performance for differentially sized particles, which will be shown in Section 4.

2. CALCULATION CONDITIONS

In this article, the Lattice Boltzmann-cellular automata (LB-CA) probabilistic model is used to simulate gas–solid flows in filtration and four different types of noncircular fibers are considered, including triangular (regular triangle) fiber, quatrefoil fiber (formed by two orthogonal ellipses), trilobal fiber (formed by three ellipses with a separation angle of 120 degrees from each other and with the same focus), and rectangular fiber (Figure 1). The computational domain of the flow field is a two-dimensional square, and a fiber is placed at the center of the flow field. The grid resolution is 256×256 for the computational domain, which has been proved to be good enough to obtain reliable flow fields. All the fibers have the same packing density α (or volume fraction, which is the ratio of the fibers' cross-sectional area to that of the computational domain for 2-D cases) and α is 4.95% in this article. In fact, our previous simulation for the elliptical fibers proved that the pressure drop ratio and capture efficiency ratio of an elliptical fiber to circular fiber are almost independent of the packing density within a wide range of 2%–15%. Particle-loaded suspension flow enters from the left boundary and is perpendicular to the fiber's principal axis. The upper and lower boundaries are periodic, and the inlet velocity remains constant: $u(y) = U$. The velocity gradient of the outlet boundary is zero, i.e., $\partial u/\partial x = \partial v/\partial x = 0$. A non-equilibrium extrapolation scheme is used in the LBM to address inlet and outlet boundary conditions. When an error in the LBM simulation results, $\sum_{j,i} |u^*_{j,i} - u_{j,i}| / \sum_{j,i} |u^*_{j,i}|$ is less than 10^{-5}, the flow field is considered to have reached a stable state, where $u_{j,i}$ is the fluid velocity of a node indexed by j in the y dimension and i in the x dimension, and the asterisk indicates the value after a time step.

It is worth noting that the Reynolds number Re is less than 1 for all cases, so the flow is regarded as an approximate Stokes flow. When the flow field is stable, particles are allowed to be injected into the flow field from the left side. The particle concentration at the inlet is kept constant, and the initial node of a solid particle at the inlet is randomly determined. The initial velocity of particles at the inlet is considered to be the same as the fluid velocity. When one particle moves onto a fiber's surface, it will be captured by this fiber. In this article, we have not considered the influence of captured particles on the flow field, i.e., particles will disappear once they are captured by fibers, and the shape of the particle collector does not change.

As is known, the mechanisms in the filtration process are very complex, such as Brownian diffusion when a small particle's random diffusion plays a dominant role, interception caused by the fiber's structure, and inertial impaction due to the collision between particles and fiber. These three mechanisms are discussed in this article. It is also well known that the particle capture processes due to different mechanisms are related to three dimensionless characteristic parameters, respectively: the Peclet number Pe, $Pe = Ud_f/D$, for Brownian diffusion-dominated filtration, where U is the average inlet velocity, d_f is the fiber diameter, D is the Brownian diffusion coefficient, $D = k_B T/(3\pi\mu d_p)$, where k_B is Boltzmann constant, and T is the temperature of gas; the intercept coefficient $R = d_p/d_f$ for interception; the Stokes number St, $St = \rho_p d_p{}^2 U/(18\mu d_f)$, for inertial impaction, where ρ_p is the particle density. It is noted here that the equivalent diameter d_f of noncircular fiber is the diameter of circular fiber with the same volume fraction (area fraction for 2-D cases).

In order to simulate the individual filtration process due to various capture mechanisms, typical values of three characteristic parameters are chosen as follows: $Pe = 235$ for Brownian diffusion, $R = 0.09375$ for interception and $St = 1.2$ for inertial impaction. Generally speaking, a fibrous filter has a higher capture efficiency for large particles (generally larger than 10 μm with a large St number) due to inertial impaction and small particles (generally less than 0.01 μm with a small Pe number) due to Brownian diffusion. However, intermediate particles (in the range of 0.1–1 μm, which are dominated by the interception mechanism) are hardly captured by the fibers. It is therefore interesting to pay more attention to the improvement in capture efficiency of intermediate particles by regulating the fiber geometry and orientation angle of noncircular fibers. In fact, when simulating cases of interception, the Brownian motion and drag force are neglected and the particles are forced to move along the streamline. In such a situation, the only factor that influences filtration is the particle

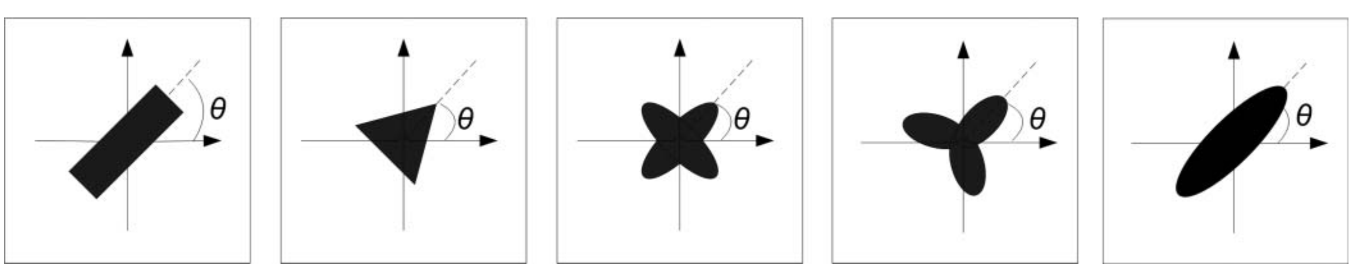

FIG. 1. Noncircular fiber arrangement (left to right: rectangular, triangular, quatrefoil, trilobal, and elliptical).

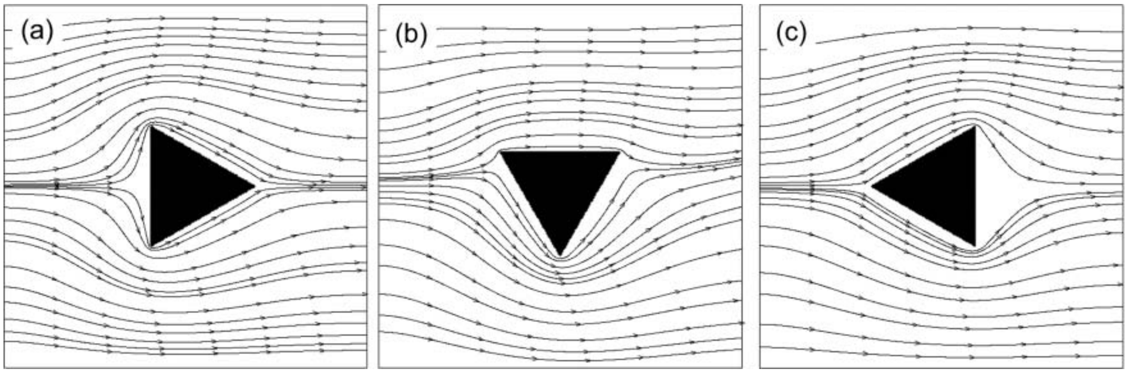

FIG. 2. Flow fields around triangular fibers with orientation angles of (a) 0°, (b) 30°, and (c) 60°.

size. When simulating cases of inertial impaction, the Brownian motion is also ignored.

It is noted that there is a certain period of rotation of a noncircular fiber with n lobes (e.g., rectangular and elliptical fibers with two lobes, triangular and trilobal fibers with three lobes, quatrefoil fiber with four lobes) on account of its particular symmetrical structure. Obviously, through simple observation, the period of rotation is $180°/n$ for a noncircular fiber with n lobes. Thus, the period of rotation for rectangular and elliptical fibers (two-lobes fiber) is $180°/2 = 90°$, $60°(= 180°/3)$ for triangular and trilobal fibers, and $45°(= 180°/4)$ for quatrefoil fibers.

3. NUMERICAL RESULTS

3.1. Triangular Fibers

As mentioned previously, three significant orientation angles (0°, 30°, and 60°) within the range of the period of rotation are investigated and the flow fields around the fibers are shown in Figure 2. As shown in Figure 2, different orientation angles have an obvious influence on the structure of flow fields. Figure 3 shows the capture efficiency of triangular fibers with different orientation angles (Figure 3a) as well as the ratios of the capture efficiency and pressure drop of triangular fibers to those of circular fibers with the same packing density (Figure 3b). In terms of the absolute capture efficiency (Figure 3a), the interceptive capture efficiency is lower than the diffusional and impaction capture efficiencies. In addition, the capture efficiency of these diffusion-dominated small particles is almost independent of the orientation angle due to the randomness of Brownian diffusion. With regard to the relative values of capture efficiency (Figure 3b), the interceptive capture efficiency with an orientation angle of 0° is higher than those of other angles, and the interceptive efficiency of triangular fibers is 2.5–3 times that of circular fibers. Factually, when the interception mechanism is dominant, the Brownian diffusion of particles is relatively weak while the effect of inertial impaction is also very small. In such cases, the particle trajectories correspond to the fluid streamlines in the entire flow field. When the distance between one particle and the fiber is smaller than the particle radius, the particle is captured. As a result, when the orientation angle is 0° (Figure 2a), the upstream zone of the fiber has a broader windward area so that the particles would be intercepted before their initial horizontal velocities change dramatically. Although the orientation angle is between 30° and 60° (Figures 2b and c), the fiber tends to be more streamlined and most particles escape from the two sides of it,

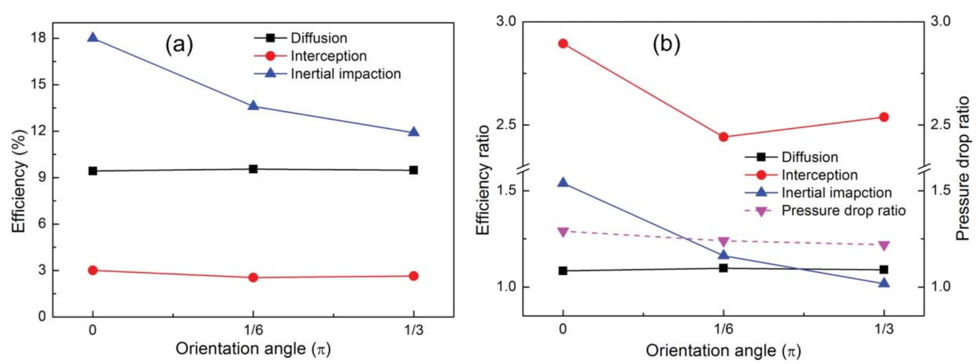

FIG. 3. Capture efficiency of triangular fibers: (a) absolute value and (b) the ratios of capture efficiency and pressure drop of triangular fibers to those of circular fibers with the same packing density.

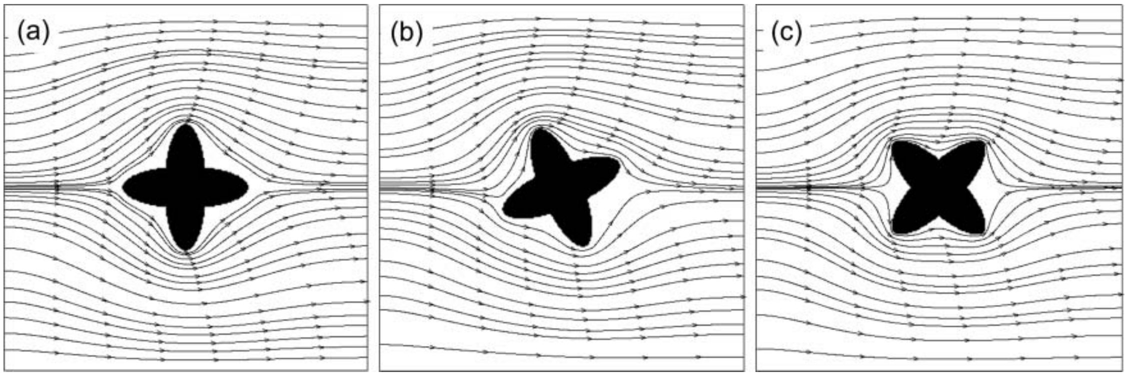

FIG. 4. Flow fields around quatrefoil fibers with an aspect ratio of 3:1 and orientation angles of (a) 0°, (b) 22.5°, and (c) 45°.

which is not conducive to particle capture. In addition, for larger particles dominated by the inertial impaction mechanism, the capture efficiency of the 0° orientation angle is also the highest, whereas that of 60° is the lowest. It is worth noting that the capture efficiencies of triangular fibers are not always much higher than those of circular fibers with the same packing density. For instance, the impaction efficiency of the 60° orientation angle is slightly smaller than that of circular fibers, which is also ascribed to much more streamlined geometry of the fiber with a 60° orientation angle. With respect to the diffusional capture efficiency, which mainly depends on the superficial area of the fiber (perimeter in 2-D cases), the triangular fiber is leading by the narrowest of margins.

As for the ratio of the pressure drop of triangular fibers to those of circular fibers (dashed line in Figure 3b), we can find that the pressure drop is greater with a 0° orientation angle; a better streamlined shape, e.g., an orientation angle of 60°, can reduce the fiber's drag force and pressure drop.

3.2. Quatrefoil Fiber

One quatrefoil fiber is formed by two orthogonal elliptical fibers. According to its symmetry properties, three orientation angles (0°, 22.5°, and 45°) are considered here (Figure 4). In addition, the shape of quatrefoil fiber is strongly affected by the aspect ratio ε (major-minor axis ratio) of component ellipses. Therefore, we mainly simulate two sets of cases in which the aspect ratio is 2:1 and 3:1, respectively. Figure 4 shows the flow fields around quatrefoil fibers under three different orientation angles when the aspect ratio is 3:1. Compared with the flow fields around the triangular fibers above, the orientation angle has a much smaller influence on the disturbance of flow fields due to its symmetrical features.

As before, the ratios of pressure drop (Figure 5a) and capture efficiency (Figure 5b) are also investigated. When the aspect ratio is bigger (i.e., the fiber is more slender), the interception area is larger, resulting in a higher pressure drop. However, the effect of the orientation angle on the pressure drop ratio is insignificant. For a fixed aspect ratio, the diffusional capture efficiency is independent of the orientation angle. Nevertheless, as the aspect ratio increases, the quatrefoil fiber has a much larger surface area (perimeter in 2-D), which leads to a significant increase in the diffusional capture efficiency (Figure 5b). For interception-dominated and inertial-dominated particles, the capture efficiencies increase as the aspect ratio increases because a bigger aspect ratio leads to a large interception range for interception and impaction. In terms of the inertial impaction mechanism, the key factor

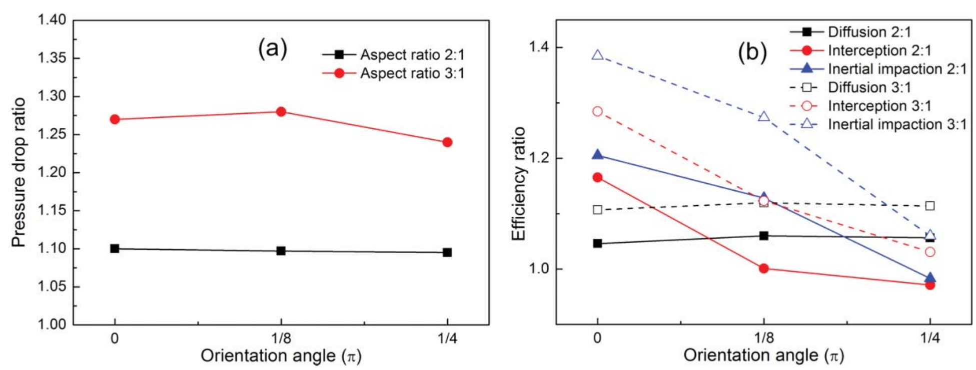

FIG. 5. The ratios of pressure drop (a) and capture efficiency (b) of quatrefoil fibers to those of circular fibers.

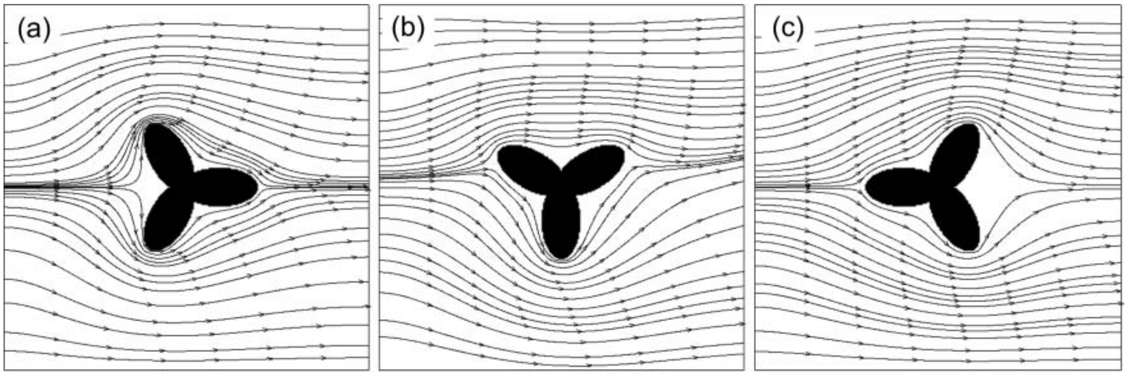

FIG. 6. Flow fields around trilobal fibers with an aspect ratio of 2:1 and orientation angles of (a) 0°, (b) 30°, and (c) 60°.

determining the capture efficiency is the windward area. As shown in Figure 4, the windward area is greatest when the orientation angle is 0°, with 22.5° second, and 45° as the smallest. Therefore, the quatrefoil fiber with a 0° orientation angle has the highest impaction efficiency, followed by the fiber with 22.5° and finally, with 45°. It is worth noting that quatrefoil fibers exhibit very good promotion of impaction efficiency, marginal promotion of diffusional efficiency and unsatisfactory promotion of the inceptive efficiency, especially with a negative effect at 45° when compared with the triangular fiber.

3.3. Trilobal Fiber

One trilobal fiber is made up of three identical ellipses with a separation angle of 120° from each other. For the sake of convenience of the simulation, we assume that these three ellipses have the same focus, which is the center of the trilobal fiber. Based on this assumption, there is a specific analytic expression for calculating the sectional area of a trilobal fiber (Fotovatia et al. 2011). Here, we also consider the influence of the aspect ratio (1.5:1 and 2:1) of the component ellipses and the orientation angle on the filtration process. Figure 6 demonstrates the flow fields when the aspect ratio is 2:1. The flow fields around trilobal fibers with different orientation angles (here 0°, 30°, and 60°) are similar to those around triangular fibers because the two types of fibers have analogous symmetrical structures.

Figure 7 presents the ratios of the systematic pressure drop and capture efficiency with different orientation angles and different aspect ratios. The pressure drop is the lowest when the orientation angle is 60°, which is ascribed to the more streamlined shape of the trilobal fiber in this case. Obviously, the variation in the pressure drop is similar to that of triangular fibers.

With respect to the capture efficiency, the diffusional efficiency of small particles is still independent of the orientation angle. As far as the interception capture is considered, the capture efficiency with a 60° orientation angle is larger than those of other angles. However, for high-inertia particles, the impaction capture efficiency is largest when the orientation angle is 0° and smallest at 60°, which is similar to the triangular fibers. Obviously, the capture efficiencies of all three capture mechanisms increase with an increase in the aspect ratio. In addition, it is worth emphasizing that when $\varepsilon = 1.5$ and $\theta = 30°$, the interceptive capture efficiency for intermediate particles of trilobal fibers is lower than that of circular fibers with the same packing density.

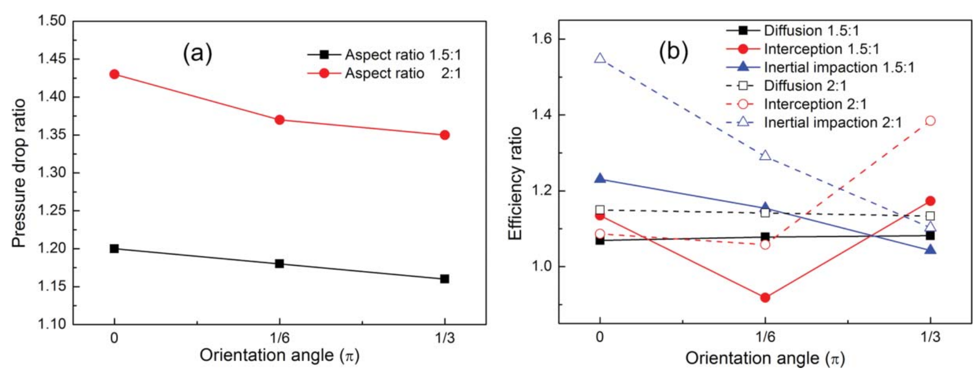

FIG. 7. The ratios of pressure drop (a) and capture efficiency (b) of trilobal fibers to those of circular fibers.

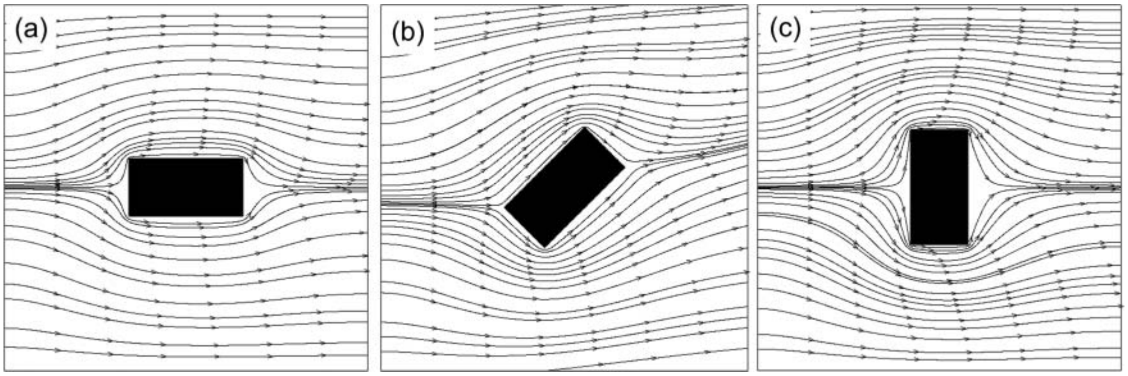

FIG. 8. Flow fields around rectangular fibers with an aspect ratio of 2:1 and orientation angles of (a) 0°, (b) 45°, and (c) 90°.

3.4. Rectangular Fiber

Two typical aspect ratios (1:1 and 2:1) of rectangular fibers are considered here and the orientation angles are 0°, 45°, and 90° (Figure 8 for the flow fields and fiber arrangements). The ratios of pressure drop and capture efficiency are investigated under the above conditions (Figure 9). In Figure 9a, when the aspect ratio is 1:1 (i.e., square fiber), the pressure drop with a 45° orientation angle is slightly larger than at other angles. In addition, the relative pressure drop for the square fiber is slightly larger than 1. However, for the rectangular fibers with a larger aspect ratio (such as 2:1 here), the pressure drop rapidly increases with the increase in the orientation angle. The pressure drop at 0° is slightly smaller than that of circular fiber, while the pressure drop at 90° is approximately 1.4 times that of circular fiber.

As shown in Figure 9b, the diffusional capture efficiency increases with the aspect ratio due to the increase in the superficial area of fibers, and this is also validated by Inagaki et al. (2001). Unlike other noncircular fibers, the capture efficiencies of rectangular fibers are not always improved when the aspect ratio is increased. For example, when the orientation angle is 0°, the interceptive and impaction capture efficiencies of rectangular fiber (2:1) are lower than those of square fibers. A similar situation is only observed for the interceptive efficiency of trilobal fiber with an orientation angle of 0°. Furthermore, it is observed that when the orientation angle is 45°, the capture efficiencies for different aspect ratios are very approximate.

3.5. Elliptical Fiber

The simulation results of the filtration of elliptical fibers are not presented here. Readers could refer to our recent publication (Wang et al. 2014). Some conclusions are summarized here for further comparison: (1) the pressure drop of elliptical fibers increases with an increase in the orientation angle and aspect ratio; (2) elliptical fibers have higher diffusional capture efficiency than circular fibers with the same packing density due to a larger surface area; (3) the diffusional capture efficiency of elliptical fibers is almost proportional to the aspect ratio while independent of the orientation angle; (4) the capture efficiency increases with the orientation angle when the interception or inertial impaction mechanism is dominant; (5) when the inertial impaction mechanism is dominant and the larger the intercept parameter is, the faster the capture efficiency increases with the orientation angle; (6) the capture efficiency of elliptical fiber is almost higher than that of circular fiber for all three mechanisms when the orientation angle of the elliptical fiber is larger than 30°, whereas the

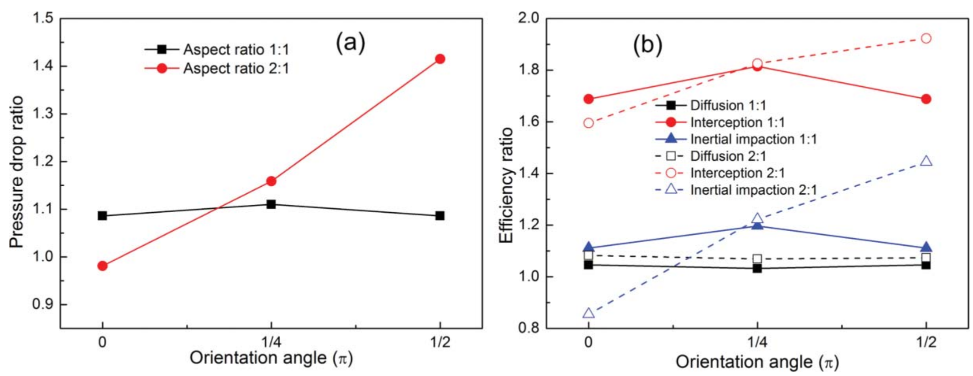

FIG. 9. The ratios of pressure drop (a) and capture efficiency (b) of rectangular fibers to those of circular fibers.

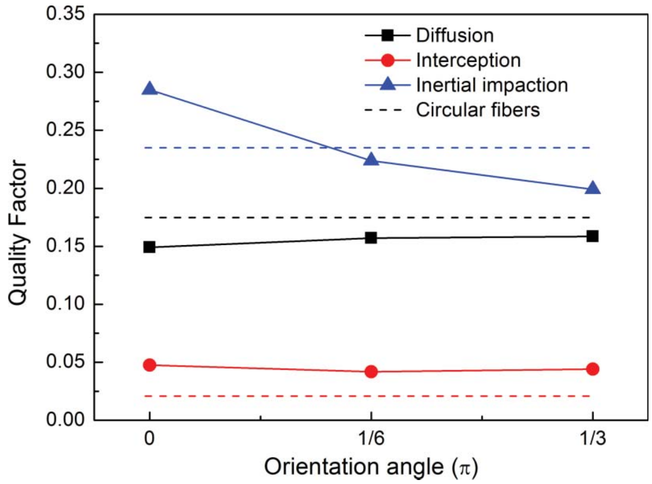

FIG. 10. The quality factor of triangular fibers together with circular fibers.

interceptive and impaction efficiencies are lower when the major axis is more parallel to the incoming flow.

4. QUALITY FACTOR

A good fibrous filter should perform with a high capture efficiency and a low pressure drop during the actual process of operation. Podgórski et al. (2006) and Wang and Pui (2009) proposed the concept of a quality factor for measuring the filtration performance and defined it as follows:

$$QF = \frac{\eta}{(1-\alpha)\cdot(2F/Re)\cdot(\rho u_0^2/2)}, \qquad [1]$$

where η is the capture efficiency, F is the dimensionless drag force of unit length fiber, Re is the Reynolds number, α is the packing density of the fiber (4.95% here), ρ is the fluid density, and u_0 is the inlet fluid velocity.

Figure 10 presents the quality factor of triangular fiber with various orientation angles due to three capture mechanisms. It demonstrates that the orientation angle has little effect on the quality factor dominated by Brownian diffusion or interception; the diffusional quality factor when $\theta = 60°$ is slightly larger because the pressure drop is lower in this situation; the interceptive quality factor when θ = 0° is also slightly larger than those at other angles because the interceptive capture efficiency is the highest when θ = 0°; and with respect to impaction-dominated cases, the quality factor when θ = 0° is much larger due to a higher impaction capture efficiency. Compared with circular fibers, triangular fibers show advantages when the interception mechanism is dominant and disadvantages when capturing diffusion-dominated small particles, in terms of the quality factor. However, for larger particles dominated by the inertial impaction mechanism, the relative quality factor depends on the orientation angle.

When considering quatrefoil/trilobal/rectangular fibers, we should take the influence of both orientation angle (θ) and aspect ratio (ε) into account. In order to investigate the effects of more extensive parameters, we supplement the simulations of larger aspect ratios, i.e., 4:1 for quatrefoil fiber, and 3:1 for trilobal and rectangular fibers. Figure 11 demonstrates the quality factor of quatrefoil fibers with various θ and ε under different operating conditions. Several conclusions can be drawn as follows. First, the quality factor decreases with the increase of ε, when Brownian diffusion is predominant. In addition, the quality factor when θ = 22.5° is slightly larger than any other orientation angle for a certain ε. Second, in general, for the intermediate and high-inertia particles, the quality factor when θ = 0° is larger than other angles. This is because the fiber's windward area is larger when θ = 0°, which leads to a broader capture range and a higher filtration performance. Third, the interceptive and impaction quality factors when θ = 0° and ε = 2 are maximized.

As for the trilobal fibers, the quality factor increases with the decrease in the aspect ratio (1.5:1) for all capture mechanisms (Figure 12) because the pressure drop is lower when ε is small. In terms of the particles dominated by diffusion or the interception mechanism, it is beneficial to improve the quality factors when θ = 60° on account of the more streamlined shape of trilobal fiber which leads to a smaller disturbance to flow fields and a lower pressure drop but a higher interception

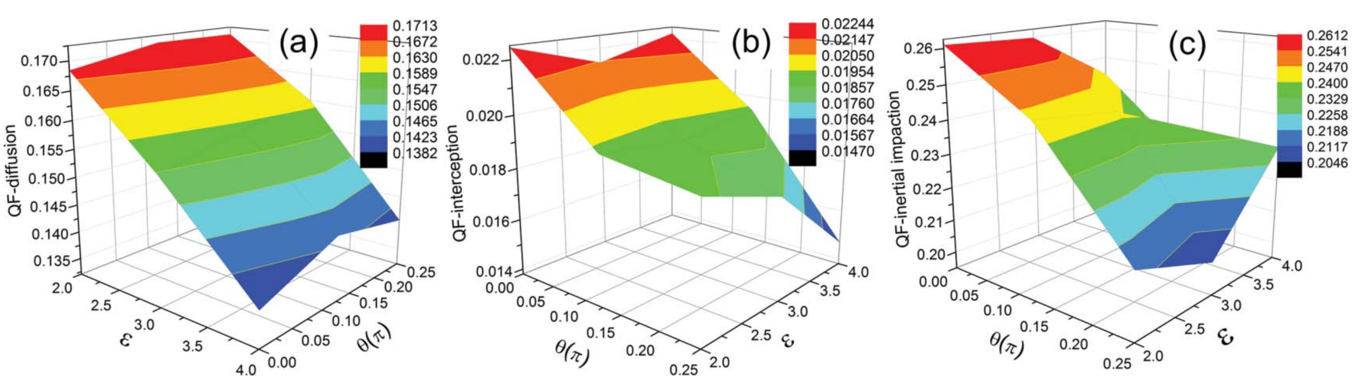

FIG. 11. The quality factor of quatrefoil fibers: (a) diffusion, (b) interception, and (c) inertial impaction.

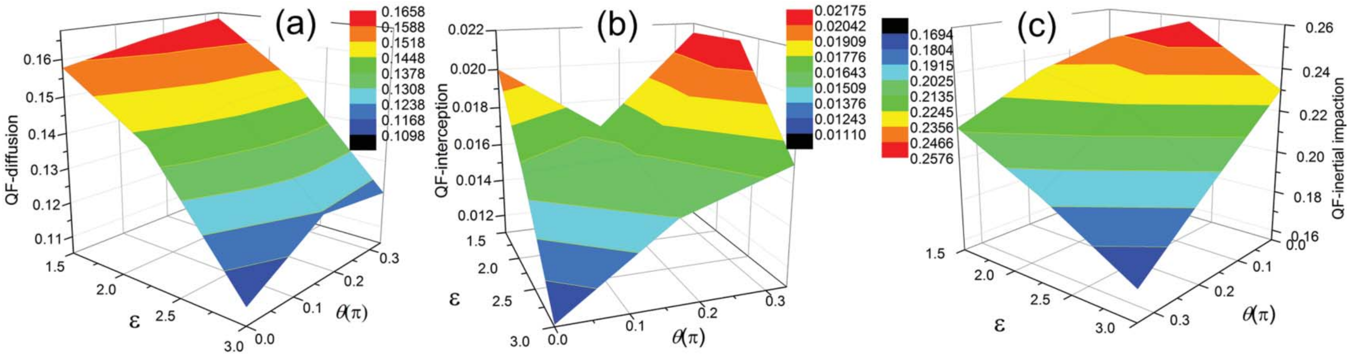

FIG. 12. The quality factor of trilobal fibers: (a) diffusion, (b) interception, and (c) inertial impaction.

capture efficiency. However, when inertial impaction is predominant, the quality factor when $\theta = 60^\circ$ is minimized and the quality factor for 0° is the largest for a certain ε. From the overall distribution of the trilobal fiber's quality factor under all conditions, the diffusional and interceptive quality factors reach a maximum when $\varepsilon = 1.5$ and $\theta = 60^\circ$, as observed in Figure 12. The quality factor reaches a maximum when $\varepsilon = 2$ and $\theta = 0^\circ$ in terms of large particles (dominated by inertial impaction).

Figure 13 presents the quality factor of rectangular fibers under various arrangements. The quality factor due to Brownian diffusion attains its maximum when $\theta = 0^\circ$ with a large aspect ratio. It is easy to understand that the fiber's superficial area increases with an increase in ε, namely for a more slender fiber. In addition, the pressure drop reaches its minimum when $\theta = 0^\circ$. Both a more slender fiber and more parallel arrangement to the incoming flow are conducive to the diffusional quality factor. However, a larger θ would lead to a greater rise in the pressure drop, which significantly decreases the quality factor. The interception filtration is similar to the diffusional filtration, i.e., a small θ (0°–45°) results in a high quality factor. However, for the inertial impaction filtration, the quality factor is larger when θ is approximately 45° on account of mutual competition between the pressure drop and capture efficiency. With the increase in the aspect ratio, the pressure drop increases faster than the impaction capture efficiency when $\theta = 45^\circ$, which leads to a decrease in the quality factor.

At this point, to explore which fiber arrangement (shape, orientation angle and aspect ratio) is conducive to a better filtration performance is a significant issue. We list the largest quality factor of all noncircular fibers (triangular, quatrefoil, trilobal, rectangle, and elliptical) and circular fiber dominated by three mechanisms in Figure 14. We find that, for small particles dominated by Brownian diffusion, the rectangular and elliptical fibers when $\varepsilon = 3$ and placed horizontally have the largest quality factor, whereas the other fibers do not show much difference in the optimal quality factor. In addition, for the intermediate and high-inertia particles dominated by interception and inertial impaction, respectively, the triangular fiber when $\theta = 0^\circ$ has the largest quality factor though the difference is not large for the impaction quality factors. Taken together, our results show that triangular and rectangular fibers could be adopted to improve the capture efficiency and quality factor of intermediate particles, which are difficult to capture using regular circular fibers.

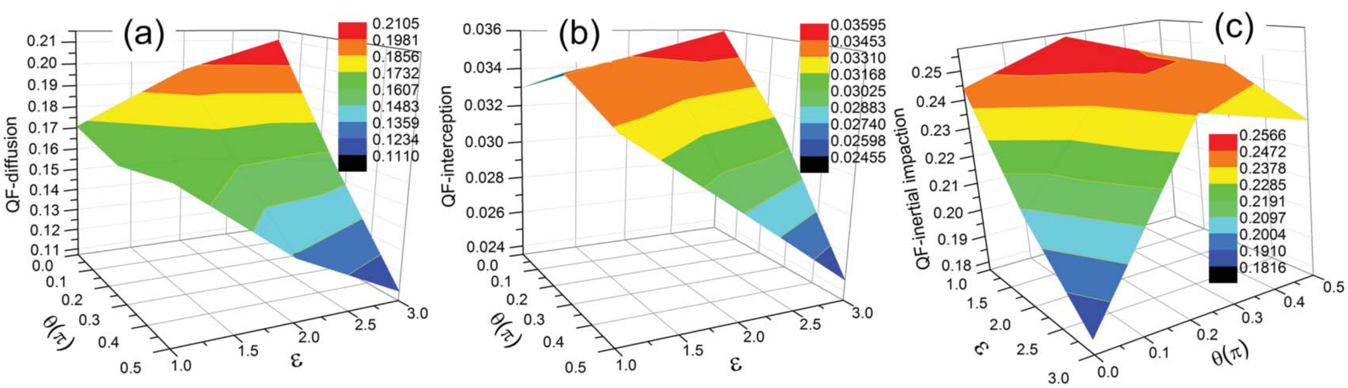

FIG. 13. The quality factor of rectangular fibers: (a) diffusion, (b) interception, and (c) inertial impaction.

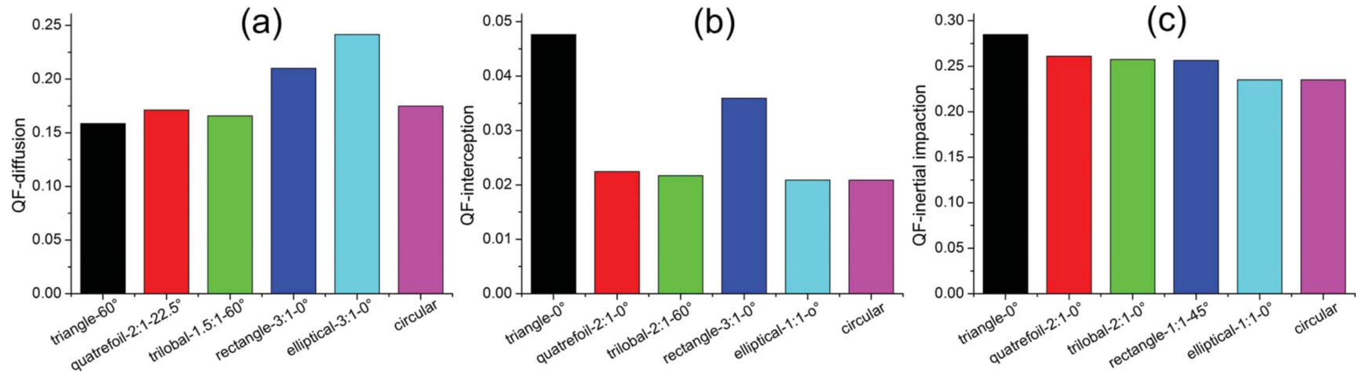

FIG. 14. The best quality factor for all types noncircular fibers dominated by three different capture mechanisms: (a) diffusion, (b) interception, and (c) inertial impaction.

5. CONCLUSION

In this article, the filtration processes of four types of noncircular fibers (triangular, quatrefoil, trilobal and rectangular fibers) with the same packing density as circular fibers are simulated by our previously developed Lattice Boltzmann-cellular automation (LB-CA) probabilistic model. Three main capture mechanisms (Brownian diffusion, interception and inertial impaction) are considered here. Meanwhile, two significant filtration performance parameters, i.e., the pressure drop and the capture efficiency, are quantitatively calculated for clean fibers during the filtration process with various fiber arrangements (cross-section shape, orientation angle, and aspect ratio). The relative pressure drop and capture efficiencies compared with circular fibers are also calculated. Then, the quality factor is chosen to characterize the filtration performance. Through comparison and analysis, several conclusions can be drawn as follows.

First, for small particles with strong Brownian diffusion, the capture efficiency is almost independent of the orientation angle of the fibers but is mainly dependent on the fiber's sectional area (perimeter in two-dimensional cases). In addition, the diffusional capture efficiencies of four types of noncircular fibers are all larger than that of circular fiber. Among these, the elliptical fiber shows an advantage in capturing diffusion-dominated particles. Second, when the interception mechanism is predominant, there is not a general rule concerning both the effects of θ and ε. However, a larger aspect ratio (for quatrefoil, trilobal, and rectangular fibers) would generally lead to a higher capture efficiency. Generally, the triangular fiber demonstrates the highest interception capture efficiency for intermediate particles. Third, in terms of high-inertia particles, the key factor to determine the capture efficiency is the windward area, and a more streamlined shape will decrease the efficiency significantly. Fourth, rectangular and elliptical fibers placed horizontally have the highest quality factor due to the diffusion mechanism, whereas for the intermediate and high-inertia particles, the triangular fiber when $\theta = 0°$ has the highest quality factor. In conclusion, through the analysis of the capture process of these noncircular fibers due to three capture mechanisms, the optimal configuration of fibers is obtained, which can provide a theoretical basis for filter design and arrangement optimization.

FUNDING

This study was financially supported by the National Natural Science Foundation of China (51276077, 51390494) and the National Key Basic Research and Development Program (2010CB227004 and 2013CB228504).

REFERENCES

Adamiak, K. (1999). Viscous Flow Model for Charged Particle Trajectories Around a Single Square Fiber in an Electric Field. *IEEE T. Ind. Appl.*, 35:352–358.

Brown, R. (1984). A Many-Fibre Model of Airflow Through a Fibrous Filter. *J. Aerosol Sci.*, 15:583–593.

Brown, R. C. (1993). *Air Filtration: An Integrated Approach to the Theory and Applications of Fibrous Filters*. Pergamon Press, New York.

Cao, Y., Cheung, C., and Yan, Z. (2004). Numerical Study of an Electret Filter Composed of an Array of Staggered Parallel Rectangular Split-Type Fibers. *Aerosol. Sci. Technol.*, 38:603–618.

Cheung, C., Cao, Y., and Yan, Z. (2005). Numerical Model for Particle Deposition and Loading in Electret Filter with Rectangular Split-Type Fibers. *Comput. Mech.*, 35:449–458.

Dhaniyala, S. (1999). An Asymmetrical, Three-Dimensional Model for Fibrous Filters. *Aerosol Sci. Technol.*, 30:333–348.

Fardi, B. and Liu, B. Y. (1992a). Flow Field and Pressure Drop of Filters with Rectangular Fibers. *Aerosol Sci. Technol.*, 17:36–44.

Fardi, B., and Liu, B. Y. (1992b). Efficiency of Fibrous Filters with Rectangular Fibers. *Aerosol Sci. Technol.*, 17:45–58.

Fotovati, S., Tafreshi, H. V., and Pourdeyhimi, B. (2011). Analytical Expressions for Predicting Performance of Aerosol Filtration Media Made up of Trilobal Fibers. *J. Hazard. Mater.*, 186:1503–1512.

Happel, J. (1959). Viscous Flow Relative to Arrays of Cylinders. *AIChE. J.*, 5:174–177.

Hosseini, S. and Tafreshi, H. V. (2011). On the Importance of Fibers' Cross-Sectional Shape for Air Filters Operating in the Slip Flow Regime. *Powder Technol.*, 212:425–431.

Inagaki, M., Sakai, K., Namiki, N., Emi, H., and Otani, Y. (2001). Influence of Fiber Cross-Sectional Shape on Filter Collection Performance. *Kagaku. Kogaku. Ronbun.*, 27:113–120.

Kirsch, A., and Fuchs, N. (1967). Studies on Fibrous Aerosol Filters—II. Pressure Drops in Systems of Parallel Cylinders. *Ann. Occup. Hyg.*, 10:23–30.

Kirsch, A., and Fuchs, N. (1968). Studies on Fibrous Aerosol Filters—III Diffusional Deposition of Aerosols in Fibrous Filters. *Ann. Occup. Hyg.*, 11:299–304.

Kirsh, V. (2011). Stokes Flow and Deposition of Aerosol Nanoparticles in Model Filters Composed of Elliptic Fibers. *Colloid J.*, 73:345–351.

Kuwabara, S. (1959). The Forces Experienced by Randomly Distributed Parallel Circular Cylinders or Spheres in a Viscous Flow at SMALL REYNOLDS NUMBERS. *J. Phys. Soc. Jpn.*, 14:527–532.

Lamb, G. E., and Costanza, P. A. (1980). Influences of Fiber Geometry on the Performance of Nonwoven Air Filters Part III: Cross-Sectional Shape. *Text. Res. J.*, 50:362–370.

Lee, K., and Liu, B. (1981). Experimental Study of Aerosol Filtration by Fibrous Filters. *Aerosol Sci. Technol.*, 1:35–46.

Lee, K., and Liu, B. (1982). Theoretical Study of Aerosol Filtration by Fibrous Filters. *Aerosol Sci. Technol.*, 1:147–161.

Liu, Z. G., and Wang, P. K. (1997). Pressure Drop and Interception Efficiency of Multifiber Filters. *Aerosol Sci. Technol.*, 26:313–325.

Ouyang, M., and Liu, B. Y. (1998). Analytical Solution of Flow Field and Pressure Drop for Filters with Rectangular Fibers. *J. Aerosol Sci.*, 29:187–196.

Podgórski, A., Bałazy, A., and Gradoń, L. (2006). Application of Nanofibers to Improve the Filtration Efficiency of the Most Penetrating Aerosol Particles in Fibrous Filters. *Chem. Eng. Sci*., 61:6804–6815.

Raynor, P. C. (2002). Flow Field and Drag for Elliptical Filter Fibers. *Aerosol Sci. Technol.*, 36:1118–1127.

Raynor, P. C. (2008). Single-Fiber Interception Efficiency for Elliptical Fibers. *Aerosol Sci. Technol.*, 42:357–368.

Regan, B. D., and Raynor, P. C. (2009). Single-Fiber Diffusion Efficiency for Elliptical Fibers. *Aerosol Sci. Technol.*, 43:533–543.

Sanchez, J. R., Rodriguez, J., Alvaro, A., and Estevez, A. (2007). The Capture of Fly Ash Particles using Circular and Noncircular Cross-Section Fabric Filters. *Environ. Prog*., 26:50–58.

Stechkina, I., and Fuchs, N. (1966). Studies on Fibrous Aerosol Filters—I. Calculation of Diffusional Deposition of Aerosols in Fibrous Filters. *Ann. Occup. Hyg.*, 9:59–64.

Stechkina, I., Kirsch, A., and Fuchs, N. (1969). Studies on Fibrous Aerosol Filters—IV Calculation of aerosol Deposition in Model Filters in the Range of Maximum Penetration. *Ann. Occup. Hyg.*, 12:1–8.

Wang, C. (1996). Stokes Flow Through an Array of Rectangular Fibers. *Int. J. Multiphase Flow.*, 22:185–194.

Wang, H., Zhao, H., Guo, Z., and Zheng, C. (2012a). Numerical Simulation of Particle Capture Process of Fibrous Filters using Lattice Boltzmann Two-Phase Flow Model. *Powder Technol.*, 227:111–122.

Wang, H., Zhao, H., Wang, K., He, Y., and Zheng, C. (2013). Simulation of Filtration Process for Multi-Fiber Filter using the Lattice-Boltzmann Two-Phase Flow Model. *J. Aerosol Sci.*, 66:164–178.

Wang, H., Zhao, H., Wang, K., Zheng, C. (2014). Simulating and Modeling Particulate Removal Processes by Elliptical Fibers. *Aerosol Sci. Technol.*, 48:207–218.

Wang, J. and Pui, D. Y. (2009). Filtration of Aerosol Particles by Elliptical Fibers: A Numerical Study. *J. Nanopart. Res.,* 11:185–196.

Wang, W., Xie, M., Wang, L. (2012b). An Exact Solution of Interception Efficiency Over an Elliptical Fiber Collector. *Aerosol Sci. Technol.*, 46:843–851.

Zhu, C., Lin, C.-H., Cheung, C. S. (2000). Inertial Impaction-Dominated Fibrous Filtration with Rectangular or Cylindrical Fibers. *Powder Technol.*, 112:149–162.